Lucie Zárybnická, Jaroslav Pokorný, Jana Machotová, Radek Ševčík, Jiří Šál, Alberto Viani (2023). Study of keto-hydrazide crosslinking effect in acrylic latex applied to Portland cements with respect to physical properties. *Construction and Building Materials*. Volume 375, 2023, 130897. DOI: 10.1016/j.conbuildmat.2023.130897

Study of keto-hydrazide crosslinking effect in acrylic latex applied to Portland cements with respect to physical properties

Lucie Zárybnická[1], Jaroslav Pokorný[2], Jana Machotová[3], Radek Ševčík[1,2], Jiří Šál[2], Alberto Viani[1]

[1]*Institute of Theoretical and Applied Mechanics of the Czech Academy of Sciences, Centre Telč, Prosecká 809/76, 190 00 Praha 9, Czech Republic*

[2]*Institute of Technology and Business, Faculty of Technology, Department of Civil Engineering, Okružní 517/10, 370 01 České Budějovice, Czech Republic*

[3]*Institute of Chemistry and Technology of Macromolecular Materials, Faculty of Chemical Technology, University of Pardubice, Studentská 573, 532 10 Pardubice, Czech Republic*

Abstract

Polymer-modified Portland-based composites are of interest for specific applications, in reason of their properties. There are different types of commercial additives and waste polymer-based materials applied to cement-based composites, however, their impacts on the environment are debatable. In this work, new acrylic latex additives with and without keto-hydrazide crosslinking have been prepared from standardly available low-cost raw monomers. The influence of their incorporation into Portland cement-based fine-grained concretes has been investigated. The obtained results indicate that the highest effect on heat flow evolution changes has been detected in the case of latexes without crosslinking. The incorporation of both latex types into produced cement composites resulted in a significant increase in open porosity connected with the gradual decrease in mechanical resistance, especially the compressive strength. On the other hand, an important mitigation of liquid water transport properties of latex-modified composites has been achieved and such properties can be tuned according to the used latex type and its concentration. The developed latex cement-based composites may find

utilization as special materials for structures or products for water-loaded constructions or in areas with high concentrations of water-soluble salts or other pollutants.

Keywords: Portland cement; Acrylic latex; Keto-hydrazide crosslinking; Water transport properties; Mechanical properties

1. Introduction

Cement-based composites are widely employed in construction [1–3]. Of the solutions adopted to improve Portland cement properties [4], the use of polymeric materials in concrete mixes is one of the most promising, bringing advantages in terms of mechanical properties, water transport properties and durability [5–9].

The concept of polymer modification for cement-based concretes and mortars is dating back to 1923, with the first patent of Cresson [10], which proposed the use of natural rubber latexes as fillers in paving materials. Since then, polymer latexes have been used to improve various properties, including the behaviour of the fresh mixtures, such as workability, adhesion to the substrate, anti-bleeding, and further properties of the hardened cement composites, e.g. flexural and tensile strength, ductility, cracking resistance, impermeability and durability [11–19]. The most commonly used types of latexes for cement-based composites are based on styrene-butadiene rubber (SBR) [20–24], styrene-acrylic ester copolymer (SAE) [20,25–28], polyacrylic ester (PAE) [29,30] and ethylene-vinyl acetate copolymer (EVA) [31–35], polyvinyl alcohol (PVA) [36] in forms of either aqueous dispersion or re-dispersible powders. SBR latex was found to help in improving flexural strength, tensile bond strength, waterproofing property, carbonation resistance, and mitigating shrinkage [20,37,38]. On one hand, SAE latex decreases the elastic modulus, but it improves the toughness of cement mortar and concrete to a larger extent [25,39]. EVA latex, the most widely used polymer in concrete,

improves the tensile bond strength, flexural strength, and toughness of hardened composites [40,41]. PAE allows the cementitious mixture to have better workability, higher flexural strength and better crack resistance [42,43]. PVA retards the hydration process, but at the same time increases the compressive strength and decreases the porosity [44].

Nowadays, acrylic latexes, i.e., water-borne acrylic polymers (pertaining to the PAE group), which consist of colloidal particles (0.05–0.5 μm in diameter) dispersed in water, are generally produced by emulsion polymerization. This procedure is a sort of free radical polymerization in an aqueous environment [45]. It represents an eco-friendly technique that yields polymer particles of spherical shape with narrow particle size distributions. Emulsion polymerization offers a great degree of versatility: polymers can be designed to meet specific application requirements, e.g. by modifying monomer composition, crosslinking density, particle size or the surface charge on latex particles. Physical and mechanical properties of water-borne acrylic polymers can be improved by chemical crosslinking [50]. Among various covalent crosslinking strategies, keto-hydrazide reaction has become popular, because it occurs only during the formation of the latex polymer film after the evaporation of a large amount of water [51] and offers the advantage of rapid, ambient-temperature networking [52]. For performing this kind of crosslinking, diacetone acrylamide (DAAM) is usually implemented during the polymer synthesis by copolymerization with basic monomers and adipic acid dihydrazide (ADH) is dissolved in the aqueous dispersion medium.

Latex-modified mortars and concretes have a porous structure in which the larger pores can be filled with polymers or sealed with continuous polymer films. In general, the effect of polymer filling or sealing increases when the polymer content or polymer cement ratio, increases. This results in reduced water absorption and water permeability [47,48]. Developing water repellent properties may be beneficial for the long-term resistance of the composites; for

example, it impairs chloride ion penetration [47], critical for the corrosion of reinforcing bars in bearing concrete structures [49].

This work focuses first on the design and synthesis of water-borne acrylic latex additives with and without covalent keto-hydrazide crosslinking in their structure. In general, the preparation of these materials is also more accessible in terms of synthesis. Second, the effect of covalent crosslinking on the hydration process, water-transport performance, physical and mechanical properties of modified fine-grained concretes was evaluated. The results indicated that the increase in the latex content, induced an increase in open porosity, accompanied by a limited reduction of compressive strength. On the contrary, a small increase in flexural strength was observed. However, the polymers helped in reducing the water intake of concrete by decreasing their absorption coefficients and moisture diffusion. Specifically, there was a decrease in water absorption coefficient, apparent moisture diffusivity and sorptivity compared to the reference. The observed changes were also function of the amount of the latex additive, but they were not influenced by crosslinking. Conversely, the capillary saturated water, which increased in comparison with the reference, and increasing the latex content, was higher in the samples containing crosslinked latex.

2. Experimental part

2.1 Materials

Acrylic latexes were synthesized from methyl methacrylate (MMA), butyl acrylate (BA), methacrylic acid (MAA), and diacetone acrylamide (DAAM). All the monomers were obtained from Merck KGaA, Germany. Disponil FES 993 (BASF, Ltd., Germany) was applied as the surfactant, and ammonium persulfate (Penta, Ltd., Czech Republic) as the initiator was used. Adipic acid dihydrazide (ADH) was chosen as the covalent crosslinker and was purchased from Merck KGaA, Germany. 2-amino-2-methyl-1-propanol AMP-95 (Sigma-Aldrich, Ltd., Czech

Republic) was used for latex alkalization. All mentioned chemicals were blended and incorporated as received without further purification.

The fine-grained concrete specimens were prepared using the ordinary Portland cement 42.5 R (CEM I), produced by Českomoravský cement, Ltd., Czech Republic and meeting the requirements specified in EN 197-1 [56]. The chemical composition and some material characteristics of the used cement type are summarized in **Tables S1** and **S2**. According to the data provided by the manufacturer, CEM I reaches considerable higher mechanical resistance, namely 9.1 MPa of bending and 59.1 MPa of compressive strength after 28-days, with respect to the EN 196-1 [57]. Silica mined aggregate (SMA) in the fractions of 0.0/0.5 mm, 0.5/1.0 mm and 0.0/2.0 mm delivered by Filtrační písky, Ltd., Czech Republic, was used as a filler material for fine-grained concrete mixes. Adequate fractions of aggregate were combined together, so smooth particle size distribution was obtained, as shown in **Figure 1**. In addition, physical properties related to the size fractions of aggregate are summarized in **Table 1**.

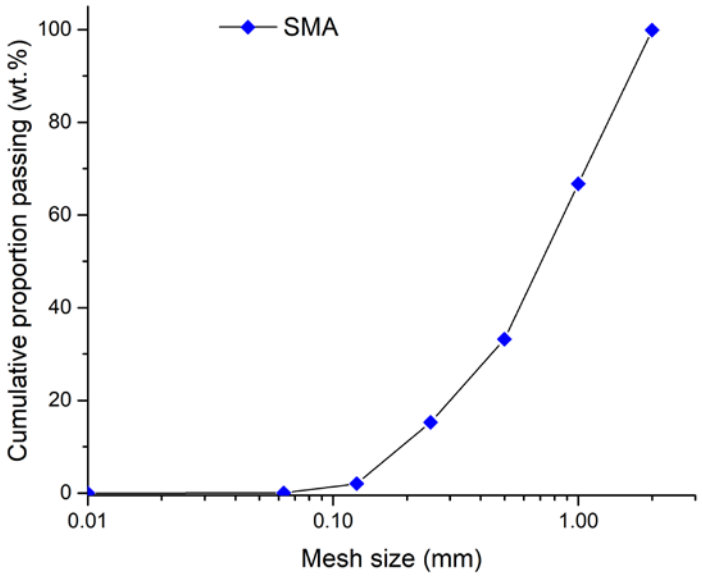

Fig. 1. Particle size distribution of SMA.

Table 1. Properties of the size fractions of SMA.

Aggregate fraction	Loose bulk density ($kg \cdot m^{-3}$)	Compacted bulk density ($kg \cdot m^{-3}$)	Specific density ($kg \cdot m^{-3}$)	Voids (%)
0.0/0.5 mm	1 424 ± 20	1 546 ± 17	2 652 ± 10	46
0.5/1.0 mm	1 515 ± 19	1 632 ± 13	2 647 ± 14	43
1.0/2.0 mm	1 538 ± 12	1 651 ± 14	2 642 ± 14	41

3.3 Preparation of samples

Synthesis of acrylic latexes

Two types of acrylic latexes were prepared by a two-step non-seeded semi-continuous emulsion polymerization technique. The latex labelled L_1 did not provide a chemical crosslinking reaction, whereas the latex labelled L_2 was designed to employ covalent keto-hydrazide crosslinking. To ensure the chemical crosslinking of latex polymer, a constant amount of DAAM (5 wt.% with respect to second step monomer feeds, which is a typical content for relevant latex compositions [55,58,59]) was incorporated into the second step, to introduce carbonyl functional groups. The proportions of individual monomers were adjusted to obtain high polymer mobility on the one hand, and non-tackiness on the other hand, in a wide temperature interval of cement hydration 5–40 °C. The specific proportions of the monomers for the synthesis of the latex L_1 were as follows: 42 g MMA, 56 g BA and 2 g MAA polymerized both in the first and second steps. In the case of the latex L_2, the specific proportions of the monomers were as follows: 42 g MMA, 56 g BA and 2 g MAA polymerized in the first step and 38 g MMA, 55 g BA, 2 g MAA and 5 g DAAM polymerized in the second step.

The latexes were synthesized in a 1000 mL glass reaction vessel under a nitrogen atmosphere at a polymerization temperature of 85 ± 1 °C. The reactor charge (consisting of distilled water,

surfactant and initiator, see **Table 2**) was placed into the reaction vessel and heated to (85 ± 1) °C. The monomer emulsion was consequently dosed into the stirred reaction vessel at a dosing rate of about 2 $mL \cdot min^{-1}$ in two steps, while a 15-minute-long period between the two dosing steps was held. The polymerization was then completed during the 2 h of the hold period. A detailed composition of the polymerization system is presented in **Table 2**. In the case of latex L_2, 10 wt.% aqueous solutions of ADH in the amount corresponding to the molar ratio ADH:DAAM = 1:2, was consequently added to the latex. Finally, the latex pH (for both samples) was adjusted to 10 with AMP-95 (50 wt.% aqueous solution).

Table 2. Composition of the polymerization system.

Composition	Reactor charge (g)	1st step monomer emulsion (g)	2nd step monomer emulsion (g)
Water	65	115	115
Disponil FES 993	0.5	7.4	7.4
Ammonium persulfate	0.4	0.4	0.4
Monomer mixture	-	100	100

Preparation of fine-grained concretes

The batching proportions of the design mix with various acrylic latex content and reference mix (REF) are summarized in **Table 3**. The ordinary concrete mix comprised 487.8 $kg \cdot m^{-3}$of Portland cement that was blended with SMA in the weight ratio of 1:3. In the rest of the mixtures, acrylic latexes in the amount of 0.5, 1.0, 1.5 and 2.0 wt. % by CEM I weight was added. The w/c ratio of 0.5 was kept constant for all prepared mixes. In the preparation of acrylic latex modified concrete specimens, water contained in latex additive was taken into account in the mix formulation.

From the presented formulations, one can see that the latex fraction is replacing the other components in the mix. The samples were designated as L**x**_**y**, where **x** is a type of latex (**1** for acrylic latex without crosslinking, **2** for acrylic latex with crosslinking) and **y** is the amount of latex in the concrete mix (in wt.%).

Table 3. Summarization of proportions of developed concrete mixes with the indication of used abbreviations.

Material	Composition ($kg \cdot m^{-3}$)								
	REF	L1_0.5	L1_1.0	L1_1.5	L1_2.0	L2_0.5	L2_1.0	L2_1.5	L2_2.0
CEM I	491	475	452	438	425	470	448	433	424
SMA	1 473	1 425	1 357	1 315	1 276	1 410	1 345	1 300	1 272
Acrylic latex	-	2.4	5	7	9	2	4	7	8
Water	247	236	223	215	207	233	221	213	207

Fresh mixtures were prepared using the mixer SP 200 (Spar, Ltd., Taiwan), disposing volume capacity of 15 L and allowing the homogenization of components within three different speed regimes. In the first step, dry components, i.e., Portland cement and silica aggregate only were blended at 1st speed regime (94 rpm) for 60 s. Then, the batch water or a blend of batch water and a latex type were continuously poured into the dry mix during 30 s intervals. The mixing continued for another 30 s with unchanged velocity. After the end of this step, mixing was interrupted to remove the dry sediment of input raw materials from the bottom of the mixing vessel. Finally, the fresh mix was homogenized at the 2nd speed regime (198 rpm) for 120 s. Fresh composites were cast into iron molds, confirming the requirements of the standard EN 12390-1 [60], in the shape of prisms with dimensions of 40×40×160 mm. Samples were cast in one step and compacted using a vibrating table (Matest, S.p.A., Italy) operating with the frequency of 40 Hz (2 400 oscillations per minute) for 1 min. Filled molds were covered by plastic foil and left in laboratory conditions at a temperature of 20 ± 1 ºC and 45 ± 5 % relative humidity. After 24 hours, specimens were demolded and stored underwater at a temperature of 20 ± 1 ºC for 6 and 27 days. In total, 12 prisms were further subjected to experimental testing. The procedure adopted to prepare the samples, which entails their immersion in water after 24 hours, prevented the elution of the monomer, since 24 hours are sufficient to form a stable film [61].

2.3 Testing procedures

Latex characterization

The solid content of the synthetized latexes was measured according to CSN EN ISO 3251 [62]. The minimum film-forming temperature (MFFT) of the latexes was determined according to ISO 2115 [63], using the MFFT-60 instrument (Rhopoint Instruments, Ltd., UK). The MFFT indicates the lowest temperature when the polymer particles have sufficient mobility and flexibility to flow together and form a continuous film. The apparent viscosity of designed additives was determined at room temperature (RT) 25±1 °C using a Brookfield LVDV-E Viscometer (Brookfield Engineering Laboratories, Inc., USA), at 100 rpm according to the CSN EN ISO 2555 [64]. The average particles size of prepared acrylic latexes was measured by dynamic light scattering (DLS) on a Coulter N4 Plus instrument (Coulter, Corp., UK) at RT. The degree of crosslinking introduced into neat latex polymers was evaluated according to gel content. For the testing, free-standing films were prepared by pouring and drying the latexes into silicone moulds. The drying of samples proceeded first at RT for a month. The gel content was determined by the extraction in a Soxhlet extractor with tetrahydrofuran (THF) for 24 h according to CSN EN ISO 6427 [65].

Fine-grained concrete constituents' characterization

According to the procedure described in EN 1097-3 [49], the bulk density of aggregate used in the loose and compacted state was determined. A vibrating table (Matest, S.p.A., Italy) with the operating frequency of 40 Hz was employed to ensure the desired compaction rate of aggregates samples. The expanded combined uncertainty of the applied method was 1.5%. For specific density measurements, the helium pycnometer AccuPyc II 1340 (Micro-Metrics Co., Ltd., France) was used. The expanded combined uncertainty of specific density determination resulted in lower than 1%. The particle size distribution of the aggregate blend was obtained

with the sieving analysis procedure described in the CSN EN 933-1 [59]. The dried representative aggregate sample was sieved through the set of sieves having a mesh size of 2.0, 1.0, 0.5, 0.25, 0.125, and 0.063 mm and shaken by vibratory device Retsch AS 200 (Retsch, GmbH, Germany).

Monitoring of hydration process

The heat signal during the setting reaction has been followed with isothermal conduction calorimetry (ICC) with a TAM-Air (TA Instruments, DE) 8-channel instrument. Powder and liquid starting components were separated in an Ad-Mix® ampoule until both were equilibrated at the measuring temperature of 25 °C. The liquid was manually injected onto the powder, defining the start of the experiment. The slurry was mixed for 120 s, and the heat flow was recorded for 7 days.

Characterization of composites

Spreading values of fresh fine-grained concretes were measured according to the EN 1015-3 [67]. Physical, strength and liquid water transport properties were accessed on hardened concretes. Bulk density was measured in accordance with the standard EN 1015-10 [68]. Open porosity was determined using the gravimetric method The standard EN 1936 [69][70]. The expanded combined uncertainty for bulk density and open porosity assessment corresponded to 1.7% and 5%, respectively. The tests were carried out on six sample replicates. Bending and compressive strength tests were performed with the hydraulic press Servo Plus Evolution (Matest, S.p.A., Italy). Prismatic samples, with dimensions 40×40×160 mm, were in the first step subjected to a three-point bending loading. On broken halves of prisms, maximum compressive forces were recorded and recalculated to compressive strengths. Compressive as well as flexural tests were performed on eight sample replicates. The expanded uncertainty for both strength determinations did not exceed 2%. The procedure of one-dimensional liquid water

transport is described in the standard EN 1015-18 [71]. On this account, the cited document introduces absorption coefficient (A) as an indicator of liquid water transport rate through the porous system of siliceous materials [72]). Further, capillary saturated water content (w_{cap}) from measured values of the tested specimen's capillary saturated and dry weight can be deduced. Apparent moisture diffusivity (X_{app}) from known absorption coefficient values and capillary saturated water content was calculated [73]. The experimental investigation was always performed on six sample replicates of each concrete type; combined expanded uncertainty was 4.3% for absorption coefficient determination, 5% in case of capillary saturated water content, and 10% for apparent moisture diffusivity assessment.

The microstructure of samples aged 28 days was investigated with a scanning electron microscope (SEM) Quanta 450 FEG (FEI, Czech Republic) using a secondary electron detector. Observations were conducted on fractured surfaces at 20 kV accelerating voltage. Samples were placed on carbon tape and gold coated with a 7 nm thick layer.

The pore size distribution was measured with a mercury intrusion porosimeter (Autopore IV 9500, Micrometrics, USA). X-ray powder diffraction (XRPD) data were collected at 40 kV and 40 mA with a Bragg–Brentano θ-θ diffractometer (Bruker D8 Advance, USA, Cu Kα radiation (λ=1.5418 Å)). Samples containing latexes were first dissolved in tetrahydrofuran and then were ground by hand in an agate mortar, sieved at 0.063 mm, and data were collected in the angular range 14–82° 2θ counting 0.4 s for each step of 0.0102° 2θ. Rietveld refinements for quantitative phase analysis (QPA) were performed with TOPAS 4.2 (Bruker AXS) implementing the fundamental parameter approach. Quantification of the amorphous phase was made possible by spiking the samples with 10 wt.% of corundum (NIST SRM 676a) as the internal standard.

3. Results and discussion

3.1 Characterization of acrylic latexes

The properties of both synthesized acrylic latexes, listed in **Table 4**, were in line with those of commercial latex binder products [74]. However, it is worth noting that the MFFT values were significantly low, which suggests high mobility and penetration ability, and favours adhesion and cohesion of the resulting composites, even at low cement application temperatures [75].

Table 4. Characteristic properties of the latexes and gel content of resulting latex polymers.

Sample	Viscosity (mPa.s)	Average particle size (nm)	MFFT (°C)	Solids (wt.%)	Gel content (wt.%)
L_1	24.4 ± 0.2	138.1 ± 2.9	0.2 ± 0.1	38.1 ± 0.1	2.9 ± 0.4
L_2	29.1 ± 0.1	147.2 ± 1.5	0.4 ± 0.2	36.8 ± 0.1	88.0 ± 2.5

The gel content expresses the level of crosslinking introduced in the polymer. It is related to several properties, like mechanical parameters and resistance to water and organic solvents. For example, the water-resistance [71–74] and tensile moduli [75–77] increase in proportion to the gel content in latex polymer. The low gel content exhibited by latex polymer L_1 is likely due to intra-particle crosslinks, i.e., crosslinking originated from chain transfer reactions that occur within the individual latex particles. The high gel content of L_2 polymer is essentially due to covalent bonds, thanks to the keto-hydrazide crosslinking [75] which proceeds between adjacent latex particles (inter-particle crosslinks). As a result, latex L_2 has the ability to form an interpenetrating chemical polymer network with enhanced cohesion.

3.2 Hydration of fine-grained concrete composites

Fig. 2 illustrates the ICC traces describing the hydration process of the studied composites. Heat evolution curves are commonly used to describe the mechanisms of hydration in Portland cement-based materials [74]. For practical purposes, they are usually divided into 3 main periods: a first one, up to the end of the induction period, the second one, corresponding to the

main hydration peak, and a third one, related to the later hydration. The main hydration reaction precedes the film formation process of acrylic latex [76]. Therefore, physical-chemical interaction between the latex particles and the reacting system may occur. This includes surface adsorption processes, such as bonding to the aggregate surface, or crosslinking of acrylic latex by Ca^{2+} ions in solution [77].

The introduction of the latex L_1 (without crosslinking) had an accelerating effect on the early stage entailing mineral dissolution (**Fig. 2**). Consequently, the main hydration was anticipated. The maximum of the acceleratory period was decreased and the rates of the later hydration reaction are lower, as also indicated by the heat of reaction curves in the inset in **Fig. 3**. Conversely, the latex L_2 (with crosslinking) had much less influence on the reaction kinetics. The results listed in **Table 5** reveal that the samples based on the latex L_2 produced almost the same heat as the reference. The differences in the total heat released during the acceleratory period may reflect compositional differences between the composites, which should correspond to microstructural changes and, in turn, differences in their mechanical performance, as the rates of hydration during the acceleratory period are controlled by the rate of C-S-H formation [78]. The second maximum of heat released (the sulfate depletion peak) became more pronounced for samples with L_2 latex (L2_1.0, L2_1.5, L2_2.0), in comparison with the reference. A similar amplification effect on cement hydration rates and total heat released has been already reported during the Portland cement hydration in the presence of carboxylate styrene-butadiene latex copolymer [79].

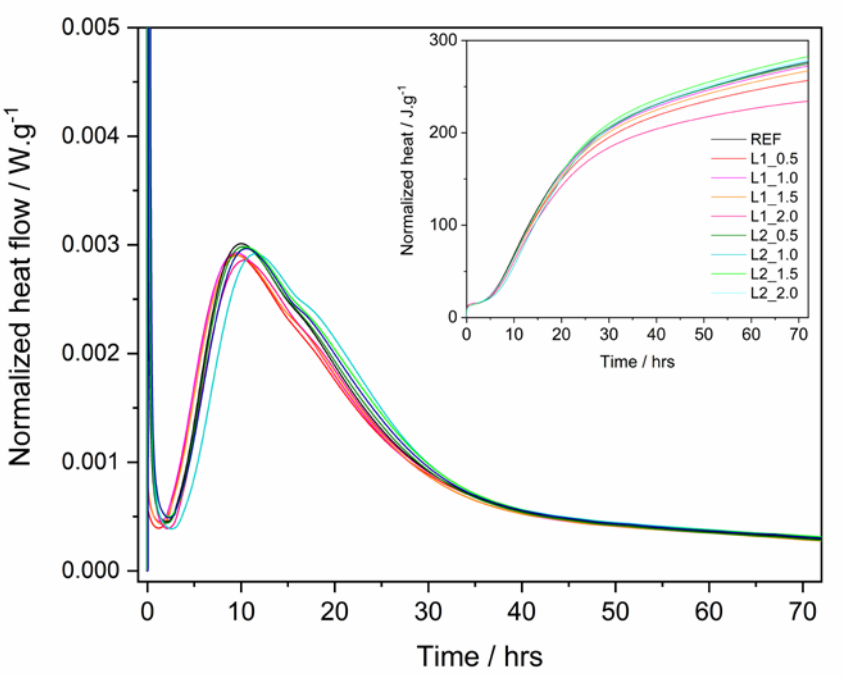

Fig. 2. Normalized heat flow evolution and Normalized heat during the hydration process by ICC.

Table 5. Heat evolution results for all samples.

Sample	Heat evolution (J)				The total amount of heat (J)
	1 hr	1 day	3 day	7 day	
REF	0.12	331.0	524.2	617.4	1 472.8
L1_0.5	0.13	311.7	478.8	512.4	1 302.9
L1_1.0	0.18	325.3	512.4	594.5	1 432.4
L1_1.5	0.17	319.4	500.2	562.3	1 382.1
L1_2.0	0.10	291.7	426.5	392.1	1 110.4
L2_0.5	0.11	329.9	521.6	612.9	1 464.6
L2_1.0	0.10	319.9	524.7	620.2	1 464.9
L2_1.5	0.13	332.4	534.2	636.4	1 503.1
L2_2.0	0.12	329.1	526.9	623.7	1 479.8

3.3 Mineralogical composition of fine-grained concrete samples

Results of XRPD are presented in **Table 6**. All samples exhibited significant and variable amounts of Ca-carbonates. Despite the CEM I can host up to 10 wt. % of limestone, the content detected in the concrete composites indicates that the samples underwent later carbonation. This

is further confirmed by the presence of all three anhydrous polymorphs including the less stable phases vaterite and aragonite. The process involves the partial removal of Ca from the C-S-H, which consequently undergo structural changes and exhibits a lower Ca/Si ratio [80]. The crystallization of the other polymorphs aragonite and vaterite has been also reported [81]. Carbonation occurred to variable extent in the samples, but a correlation between the partial consumption of the C-S-H and the formation of Ca-carbonates is observed as a decrease in amorphous fraction with the increase in the amount of carbonates. In this respect, the sample L2_2.0 is illustrative, since a similar amount of heat was released at the end of the reaction and it exhibits similar content in portlandite with respect to the other L_2 samples, but by far the lowest amount of C-S-H. This can be explained by considering a more intensive carbonation, as its higher amount of Ca-carbonates would suggest.

An increase in portlandite and amorphous/para-crystalline phases and depletion of clinker minerals may be taken as indicators of the degree of hydration. In this view, it can be noticed that specimens with L_1 and L_2 additives showed a significant increase in the weight fraction of portlandite, respect to the reference, which indicates a positive effect on the early hydration, in agreement with the respective calorimetric curves. Less straightforward is the analysis of the effect of latex addition on the amount of calcium silicate hydrates (essentially detected as amorphous phase), due to the variable extent of carbonation discussed above.

Table 6. Results of QPA (as wt.%) for the samples after 28 days.

Sample	REF	L1_0.5	L1_1.0	L1_1.5	L1_2.0	L2_0.5	L2_1.0	L2_1.5	L2_2.0
Belite	4.7	3.0	2.9	4.3	2.7	2.5	2.9	2.7	3.7
Alite	1.8	1.4	0.8	1.9	1.1	0.9	0.9	0.5	2.6
Aluminate	0.2	0.3	0.3	0.8	0.2	0.2	0.4	0.2	0.8
Ferrite	1.8	0.7	1.1	1.6	0.7	0.4	0.8	0.7	1.9
Ettringite	2.1	2.6	3.1	2.3	2.5	2.4	2.9	3.2	2.5
Portlandite	7.9	11.2	15.2	11.7	12.3	10.7	13.0	15.1	12.8
Hydrogarnet	1.1	1.1	1.0	0.8	1.1	1.0	0.9	0.9	0.6
Gypsum	0.4	0.2	0.5	0.3	0.4	0.9	0.4	0.3	0.3
Calcite	6.0	3.6	8.0	10.5	5.9	4.8	5.4	5.3	12.2

Aragonite	7.1	2.3	4.2	6.9	3.1	3.8	3.6	4.8	7.9
Vaterite	5.0	3.0	5.4	5.4	3.5	4.0	3.4	5.1	6.9
Amorphous	62.0	71.0	57.0	54.0	66.0	68.0	65.0	61.0	48.0
Carbonates	18.1	8.9	17.6	22.8	12.5	12.7	12.3	15.2	27.0

3.4 Observation of microstructure

A gallery of SEM images from selected samples is depicted in Fig. 3. The well-compacted structure of the reference sample is illustrated in Fig. 3a. In the matrix, C-S-H and $Ca(OH)_2$ phases surround the tabular crystals of gypsum [82]. In contrast, sample L2_2.0 represents a more heterogeneous microstructure with clearly visible larger voids and with the presence of higher amounts of needle-like ettringite crystals [83]. In Fig. 3c-d, collected at higher magnifications, the presence of latex polymer was confirmed. The formation of bridging between latex and the component of the cementitious matrix is illustrated in Fig. 3c. The thin layer of polymeric latex film, partially covering ettringite crystals, is visible in Fig. 4d. These features are common to cement mortars and/or concretes composites containing various types of polymers [84]. It is worth noting that the presence of continuous, and even discontinuous, polymer films may have a beneficial effect on the strengthening of microstructure [84].

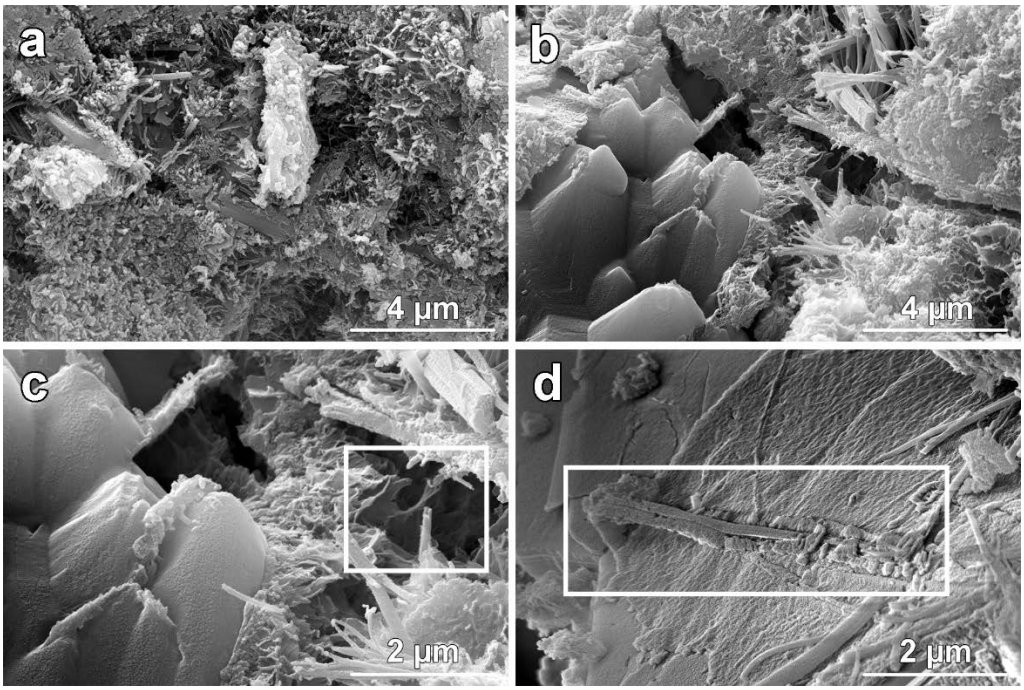

Fig. 3. SEM pictures for samples, a - REF, b - L2_2.0, c - detail of bridging, d - ettringite covered by latex L2 on aggregate grain.

3.5 Physical properties

The basic structural properties of the concrete composites and reference concrete are summarized in **Table 7**. An overall trend towards the slight increase of bulk density and the decline of open porosity from 7 to 28 days, due to the increasing extent of hydration reaction, is observed. The incorporation of both latex L_1 and L_2 reduced the bulk density with respect to the reference; the amount of this change obviously increased with the latex content, reaching 12.7% and 13.6% for the samples L1_2.0 and L2_2.0, respectively. Conversely, the open porosity measured at 7 and 28 days increased as a consequence of the introduction of both latex additives. The average open porosity of 18.1% for the reference material at 28 days (in line with literature values [85]), was raised to 28.2% and 27.6% in L1_2.0 and L2_2.0, respectively. Again, the difference with respect to the reference, increased increasing the amount of latex introduced in the mix. The two latex types had a similar effect on porosity within the error of the measurement. Higher porosity, observed also during SEM observations (Fig. 3a-b), upon

the introduction of polymer dispersions is well-known in the literature and has been attributed to the formation of micro-bubbles during concrete mixing [86,87].

Table 7. Basic structural properties of reference and latex modified concretes.

Sample	Bulk density ($kg.m^{-3}$)		Open porosity (%)	
Days	7	28	7	28
REF	2 004 ± 18	2 065 ± 25	18.4 ± 0.6	18.1 ± 0.9
L1_0.5	1 957 ± 27	2 008 ± 18	21.9 ± 1.0	21.5 ± 0.8
L1_1.0	1 867 ± 30	1 878 ± 29	24.9 ± 0.9	24.2 ± 1.0
L1_1.5	1 822 ± 20	1 849 ± 26	26.8 ± 0.8	26.3 ± 0.7
L1_2.0	1 787 ± 23	1 803 ± 14	28.7 ± 1.3	28.2 ± 1.3
L2_0.5	1 983 ± 36	1 971 ± 34	22.3 ± 0.8	21.9 ± 1.0
L2_1.0	1 897 ± 21	1 905 ± 25	24.6 ± 1.2	24.0 ± 0.9
L2_1.5	1 804 ± 16	1 836 ± 26	27.9 ± 0.8	27.2 ± 1.1
L2_2.0	1 760 ± 35	1 784 ± 18	28.3 ± 0.9	27.6 ± 0.8

3.6 Strength characteristics

Flexural and compressive strength, are important material characteristics with respect to the performance of cementitious materials [88,89]. The results of mechanical performance tests measured at 7 and 28-days on the water-cured fine-grained concrete are listed in **Table 8.**

Samples with different addition of the acrylate latex L_1 without covalent crosslinking reached 81.8% (L1_0.5), 66.4% (L1_1.0), 50.0% (L1_1.5) and 47.0% (L1_2.0) of the compressive strength measured after 28 days in the reference. The composite incorporating the lowest amount of the latex L_1 (sample L1_0.5) performed sensibly better than the homologue containing latex L_2 with covalent crosslinking. However, this difference vanished with the higher latex contents, and samples with both latex types performed similarly. A reduction in strength, in particular of compressive strength, has been already documented in the case of cement-based composites containing latex additives [90,91]. This behaviour was observed for several polymers, whereas a more heterogeneous picture emerged when the flexural strength is considered [92]. Moreover, there are some indications of a dependence of the flexural strength

on the amount of polymer additive. Ismail et al. [93], for example, found that at 2 wt.% and 3 wt.% of polymer additive, the composite performed better than the reference, but the contrary occurred for samples containing lower and higher additive amounts (up to 10 wt.%).

For the studied samples, the flexural strength improved or was similar to the reference at low content of latex (0.5 wt.%). The better results obtained from the samples L2_0.5 could be attributed to the presence of keto-hydrazide crosslinking, which is known to improve the elastic properties of the film [94]. Anyway, for higher latex contents, the flexural strength decreased increasing the weight fraction of the polymer. Notwithstanding the role of chemical interaction between the polymer, the reaction products and the cement phases, the detrimental effect of air entrapment during mixing has been found to play a major role in determining the poorer mechanical performance of the composites [95]. Improvements may be obtained by incorporating other additives, like antifoaming agents, and/or adopting a mixed curing method (wet and dry air) [92]. Nonetheless, polymer-modified concrete usually exhibits a better long term performance and durability [92]. Indications in this respect can be gained from the measurements of parameters related to the fluid transport in the concrete volume, reported in the next sections.

Table 8. Mechanical properties for samples after 28 days, the standard deviation was up to 2%

Sample	Compressive strength (MPa)		Flexural strength (MPa)	
Days	7	28	7	28
REF	42.3 ± 1.5	56.0 ± 1.2	6.8 ± 1.9	8.2 ± 1.6
L1_0.5	36.6 ± 1.0	45.8 ± 1.9	6.7 ± 1.4	8.2 ± 1.8
L1_1.0	29.1 ± 1.7	37.2 ± 1.8	5.8 ± 1.7	6.7 ± 1.5
L1_1.5	24.5 ± 1.6	28.0 ± 1.3	5.1 ± 1.1	5.7 ± 1.2
L1_2.0	19.6 ± 1.2	26.3 ± 0.9	4.9 ± 1.3	6.0 ± 2.0
L2_0.5	37.0 ± 1.4	40.0 ± 1.5	7.1 ± 1.5	8.3 ± 1.1
L2_1.0	28.7 ± 2.0	35.4 ± 1.7	6.3 ± 2.0	6.9 ± 2.0
L2_1.5	25.2 ± 1.3	29.2 ± 1.1	5.5 ± 1.8	6.2 ± 2.0
L2_2.0	20.5 ± 1.6	27.9 ± 1.4	4.8 ± 1.0	6.3 ± 1.8

3.7 Pore size distribution

Fig. 4 illustrates the cumulative pore size distribution of the composites and the reference material after 28-days of curing. Owing to the entrapment of air during mixing, mentioned before, the composites exhibit a higher amount of big pores compared to the reference, in line with the above-reported SEM observations. Large pores are known to have an adverse effect on strength [96]. All pore sizes are more abundant in the composites, with a gradual increase with the amount of polymer added to the mix. This is in agreement with the reported trend in the mechanical properties. A difference is observed between the samples incorporating crosslinked and not crosslinked latex; the former exhibiting a lower amount of pores in the range of sizes covered. Since these samples also exhibited slightly better mechanical performance, this is confirming that the strength is largely controlled by the porosity.

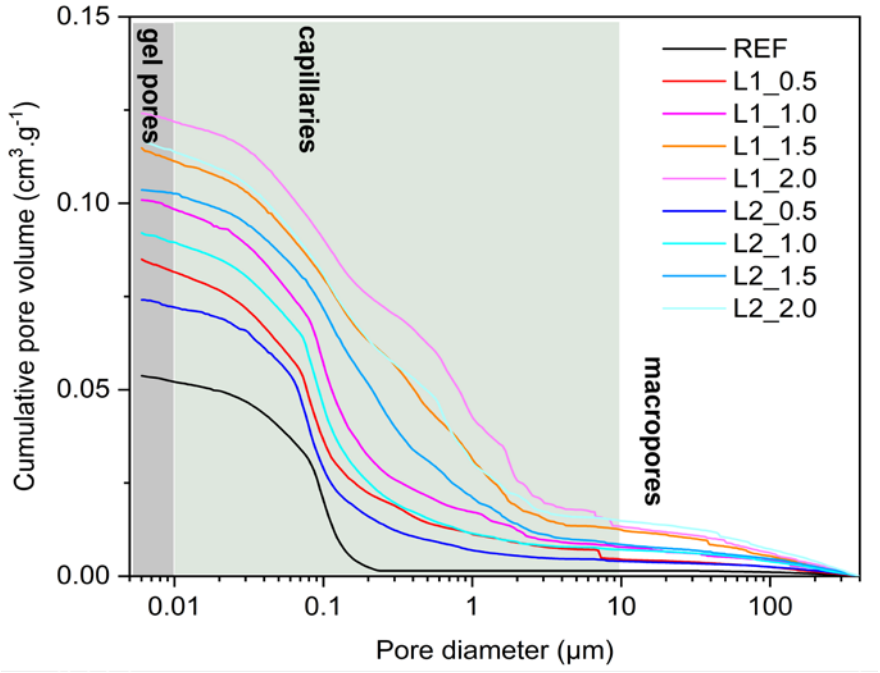

Fig. 4. Pore size distribution of concretes with different latex content.

3.8 Liquid water transport

Table 9 summarizes the results of measurements of liquid water transport properties, such as water absorption coefficient, capillary saturated water content, and apparent moisture

conductivity, conducted on the investigated samples after 7 and 28 days. Notably, despite their higher porosity, the composites exhibited a lower water absorption coefficient compared to the reference. Moreover, the amelioration was enhanced by the increase in latex content with an improvement at 28 days > 42% for both L1_2.0 and L2_2.0. The same trend was also found in a study [97] where the water absorption coefficient was monitored over time for different acrylic latexes.

The increase in the open porosity increasing the latex content, discussed in the previous section, adversely affected the capillary saturated water content (w_{cap}). However, the reduced absorption coefficients indicated that the propagation of the wet front was significantly reduced in the modified concrete. This effect should be related to the presence of the hydrophobic polymer film on the surface of pores and capillaries, hindering the water movement induced by the capillary forces [98]. The gain in water absorption coefficient was somewhat limited by the small amount of polymer dispersion introduced in the mix, since it is known that for the amounts as low as 1-2 wt%, the distribution within the concrete volume is rather inhomogeneous and affects only a limited fraction of the capillary pores [98].

The further beneficial effect of polymer addition was the reduction in apparent moisture diffusivity (X_{app}). Compared to reference concrete, the decrease reached 85.4% and 83.4% at 28 days, for L_1 and L_2, respectively. All in all, the results of dynamic tests of water and moisture transport consistently indicate that the application of both latex types may be of advantage for the concrete durability in the case of structures in direct contact with water (such as swimming pools, damps, etc.), or structures suffering from the combined action of water and, for example, water-soluble salts, like desks of bridges or drainage pipes.

In this respect, the sorptivity coefficient is a fundamental indicator for the prediction of concrete's service life as a structural material [99]. A lower sorptivity is correlated with improved durability. The results in Table 7 confirmed a significant decrease in sorptivity

compared to the reference material, with improved performance with increasing latex content. A similar trend has also been found for polyacrylic ester emulsion (PEE) latexes [100], whereas for SBR, the sorptivity increased in the interval 1-4 wt.% of polymer content. In the investigated samples, as for most of the other properties, the latex types L_1 and L_2 performed similarly with respect to sorptivity.

Table 9. One-dimensional liquid water transport properties.

Sample	Water absorption coefficient ($kg.m^{-2}.s^{-1/2}$)		Capillary saturated water content ($kg.m^{-3}$)		Apparent moisture diffusivity ($\times 10^{-8}\ m^2.s^{-1}$)		Sorptivity ($\times 10^{-5}\ m.s^{-1/2}$)	
Days	7	28	7	28	7	28	7	28
REF	0.021	0.019	158.0	154.7	1.77	1.51	2.10	1.90
L1_0.5	0.018	0.018	181.6	177.8	1.08	1.07	1.89	1.84
L1_1.0	0.015	0.014	188.2	192.6	0.66	0.49	1.53	1.35
L1_1.5	0.014	0.013	218.9	214.0	0.42	0.36	1.42	1.28
L1_2.0	0.011	0.011	231.6	228.5	0.26	0.22	1.18	1.06
L2_0.5	0.019	0.018	185.3	183.2	0.11	0.96	1.93	1.79
L2_1.0	0.015	0.014	209.9	200.4	0.49	0.50	1.47	1.42
L2_1.5	0.013	0.013	223.1	218.6	0.33	0.35	1.28	1.29
L2_2.0	0.012	0.012	243.1	235.3	0.24	0.25	1.20	1.18

Conclusion

The acrylic latex-based additives with and without covalent crosslinking were designed and synthesized in this work. The following conclusions can be made based on the experimental data collected from the produced polymer-concrete composites:

- Both latexes possessed low minimum film-forming temperature which is beneficial for their effective penetration and mobility, improving adhesion and cohesion of the cement-based composites.
- During the cement hydration, with respect to the reference concrete, in the composites containing latex without crosslinking, the first reaction step, entailing mineral dissolution,

was anticipated, with overall anticipation of the main hydration stage. Nonetheless, the rates of the later hydration reaction decreased. This resulted in a lower amount of heat released, which also decreased with the increase in the amount of latex. The hydration reaction in cement-based composites containing latex with crosslinking was more similar to the reference.

- The mineralogical analysis indicated that both polymers promoted the formation of portlandite, with a tendency towards an increase with an increase in latex content. The calcium silicate hydrate was affected by partial carbonation of the matrix in all samples (including the reference), preventing from a detailed analysis of the effect of latex on this product of hydration.
- Incorporation of both crosslinked and not crosslinked acrylic latex types brought about a gradual decrease in bulk density of concrete, which was related to the increase in open porosity, proportional to the latex additive content. This is a well-known effect due to the entrapment of air during mixing and resulted in an increase in the fraction of large capillaries and macropores in the function of the latex content, with a lower increase for the samples containing latex with crosslinking.
- The higher porosity was related to a reduction in compressive strength, which reached 47.0% and 49.8% of residual strength with respect to REF at 28-days, for the samples containing 2 wt.% of latex without and with crosslinking, respectively. The flexural strength improved or was similar to the reference at low content of latex, but for higher contents, it decreased increasing the weight fraction of the polymer.
- Significant improvements were observed in the one-dimensional liquid water transport ability of concrete upon the addition of both polymer modifiers. Although increased polymer dosages decrease the absorption coefficient values by more than 26% and 42% at 1.0 and 2.0 wt.%, respectively, for both latex types at 28 days, the apparent moisture

diffusivity decreased by more than 65% (1.0 wt.%) and 80% (2.0 wt.%) compared to traditional concrete. Relevant improvement (> 80%) was also observed for sorptivity, which is a good proxy for concrete durability in aggressive environments.

The experimental data suggested that the obtained cement-based composites may perform better in contexts where the structures are in direct contact with water, such as dams, swimming pools, or may be subjected to corrosion effects connected with the presence of water and/or moisture, like bridge desks, drainage troughs etc.

Acknowledgment

The authors gratefully acknowledge support from the Institute of Technology and Business under project SVV … and the Czech Academy of Sciences, Institute of Theoretical and Applied Mechanics-RVO 68378297.

References

[1] A. Horvath, Construction materials and the environment, Annu. Rev. Environ. Resour. 29 (2004) 181–204.

[2] B. Cwalina, Biodeterioration of concrete, brick and other mineral-based building materials, Underst. Biocorrosion. (2014) 281–312.

[3] A. Mendez, T.F. Morse, F. Mendez, Applications of embedded optical fiber sensors in reinforced concrete buildings and structures, in: Fiber Opt. Smart Struct. Ski. II, International Society for Optics and Photonics, 1990: pp. 60–69.

[4] R.J. Flatt, Conclusions and outlook on the future of concrete admixtures, in: Sci. Technol. Concr. Admixtures, Elsevier, 2016: pp. 527–530.

[5] R. Bedi, R. Chandra, S.P. Singh, Mechanical properties of polymer concrete, J. Compos. 2013 (2013).

[6] S. Fallah, M. Nematzadeh, Mechanical properties and durability of high-strength concrete containing macro-polymeric and polypropylene fibers with nano-silica and silica fume, Constr. Build. Mater. 132 (2017) 170–187.

[7] L. Li, R. Wang, Q. Lu, Influence of polymer latex on the setting time, mechanical properties and durability of calcium sulfoaluminate cement mortar, Constr. Build. Mater. 169 (2018) 911–922.

[8] M.M. Al-Zahrani, M. Maslehuddin, S.U. Al-Dulaijan, M. Ibrahim, Mechanical properties and durability characteristics of polymer-and cement-based repair materials, Cem. Concr. Compos. 25 (2003) 527–537.

[9] W. Ferdous, A. Manalo, H.S. Wong, R. Abousnina, O.S. AlAjarmeh, Y. Zhuge, P. Schubel, Optimal design for epoxy polymer concrete based on mechanical properties and durability aspects, Constr. Build. Mater. 232 (2020) 117229.

[10] L. Cresson, Improved manufacture of rubber road-facing, rubber-flooring, rubber-tiling or other rubber-lining, Br. Pat. 191 (1923) 12.

[11] E. Sakai, J. Sugita, Composite mechanism of polymer modified cement, Cem. Concr. Res. 25 (1995) 127–135.

[12] H. Bilal, T. Chen, M. Ren, X. Gao, A. Su, Influence of silica fume, metakaolin & SBR latex on strength and durability performance of pervious concrete, Constr. Build. Mater. 275 (2021) 122124.

[13] U. Ali, S. Shahid, S. Ali, Combined effects of styrene–butadiene rubber (SBR) latex and recycled aggregates on compressive strength of concrete, J. Rubber Res. (2021) 1–14.

[14] J. Wongpa, S. Koslanant, P. Thongsanitgarn, W. Chalee, Effects of Para Rubber Latex on Workability, Compressive Strength and Water Permeability of Normal Strength Concrete, Mahasarakham Int. J. Eng. Technol. 7 (2021) 61–66.

[15] J. Hot, H. Bessaies-Bey, C. Brumaud, M. Duc, C. Castella, N. Roussel, Adsorbing polymers and viscosity of cement pastes, Cem. Concr. Res. 63 (2014) 12–19. https://doi.org/https://doi.org/10.1016/j.cemconres.2014.04.005.

[16] X.-M. Kong, C.-C. Wu, Y.-R. Zhang, J.-L. Li, Polymer-modified mortar with a gradient polymer distribution: Preparation, permeability, and mechanical behaviour, Constr. Build. Mater. 38 (2013) 195–203. https://doi.org/https://doi.org/10.1016/j.conbuildmat.2012.07.080.

[17] L.K. Aggarwal, P.C. Thapliyal, S.R. Karade, Properties of polymer-modified mortars using epoxy and acrylic emulsions, Constr. Build. Mater. 21 (2007) 379–383. https://doi.org/https://doi.org/10.1016/j.conbuildmat.2005.08.007.

[18] A. Jenni, R. Zurbriggen, L. Holzer, M. Herwegh, Changes in microstructures and physical properties of polymer-modified mortars during wet storage, Cem. Concr. Res. 36 (2006) 79–90. https://doi.org/https://doi.org/10.1016/j.cemconres.2005.06.001.

[19] H. Ma, Z. Li, Microstructures and mechanical properties of polymer modified mortars under distinct mechanisms, Constr. Build. Mater. 47 (2013) 579–587. https://doi.org/https://doi.org/10.1016/j.conbuildmat.2013.05.048.

[20] R. Wang, P.-M. Wang, X.-G. Li, Physical and mechanical properties of styrene–butadiene rubber emulsion modified cement mortars, Cem. Concr. Res. 35 (2005) 900–906.

[21] K. Sun, S. Wang, L. Zeng, X. Peng, Effect of styrene-butadiene rubber latex on the rheological behavior and pore structure of cement paste, Compos. Part B Eng. 163 (2019) 282–289.

[22] Z. Yang, X. Shi, A.T. Creighton, M.M. Peterson, Effect of styrene–butadiene rubber latex on the chloride permeability and microstructure of Portland cement mortar, Constr. Build. Mater. 23 (2009) 2283–2290.

[23] E.K. Soni, Y.P. Joshi, Performance analysis of styrene butadiene rubber-latex on cement concrete mixes, J. Eng. Res. Appl. 3 (2014) 838–844.

[24] A.S. Ali, H.S. Jawad, I.S. Majeed, Improvement the properties of cement mortar by using styrene butadiene rubber polymer, J. Eng. Dev. 16 (2012) 61–72.

[25] R. Wang, P. Wang, Function of styrene-acrylic ester copolymer latex in cement mortar, Mater. Struct. 43 (2010) 443–451.

[26] X. Zhang, G. Li, Z. Song, Influence of styrene-acrylic copolymer latex on the mechanical properties and microstructure of Portland cement/Calcium aluminate cement/Gypsum cementitious mortar, Constr. Build. Mater. 227 (2019) 116666.

[27] H.A. Abdel-Rahman, M.M. Younes, M.M. Khattab, Effect of waste glass content on the physico-chemical and mechanical properties of styrene acrylic ester blended cement mortar composites, Polym. Compos. 39 (2018) 985–996.

[28] R. Wang, L. Yao, P. Wang, Mechanism analysis and effect of styrene–acrylate copolymer powder on cement hydrates, Constr. Build. Mater. 41 (2013) 538–544.

[29] C. Jiang, S. Huang, P. Gao, D. Chen, Experimental study on the bond and durability properties of mortar incorporating polyacrylic ester and silica fume, Adv. Cem. Res. 30 (2018) 56–65.

[30] C. Jiang, X. Zhou, S. Huang, D. Chen, Influence of polyacrylic ester and silica fume on the mechanical properties of mortar for repair application, Adv. Mech. Eng. 9 (2016) 1687814016683856.

[31] C.E.M. Gomes, O.P. Ferreira, M.R. Fernandes, Influence of vinyl acetate-versatic vinylester copolymer on the microstructural characteristics of cement pastes, Mater. Res. 8 (2005) 51–56.

[32] D.A.D. Silva, H.R. Roman, P.J.P. Gleize, Evidences of chemical interaction between EVA and hydrating Portland cement, Cem. Concr. Res. 32 (2002) 1383–1390.

[33] C. Shi, X. Zou, P. Wang, Influences of ethylene-vinyl acetate and methylcellulose on the properties of calcium sulfoaluminate cement, Constr. Build. Mater. 193 (2018) 474–480.

[34] Y. Jin, D. Stephan, Hydration kinetics of Portland cement in the presence of vinyl acetate ethylene latex stabilized with polyvinyl alcohol, J. Mater. Sci. 53 (2018) 7417–7430.

[35] A.M. Betioli, J. Hoppe Filho, M.A. Cincotto, P.J.P. Gleize, R.G. Pileggi, Chemical interaction between EVA and Portland cement hydration at early-age, Constr. Build. Mater. 23 (2009) 3332–3336.

[36] S. Lee, E.A. Benson, W.M. Kriven, Preparation of Portland cement components by poly (vinyl alcohol) solution polymerization, J. Am. Ceram. Soc. 82 (1999) 2049–2055.

[37] P.M. Wang, Q. Xu, J. Stark, Mechanical properties of styrene–butadiene emulsion modified cement mortar used for repair of bridge surface, J Build Mater. 4 (2001) 1–6.

[38] R. Wang, P.M. Wang, Physical properties of SBR latex-modified mortar under different curing conditions, J. Chinese Ceram. Soc. 37 (2009) 2118–2123.

[39] W.G. Wong, P. Fang, J.K. Pan, Dynamic properties impact toughness and abrasiveness of polymer-modified pastes by using nondestructive tests, Cem. Concr. Res. 33 (2003) 1371–1374.

[40] G.F. Zhang, P.M. Wang, J.G. Wu, Influence of polymer powder on the bulk density and capillary water adsorption of cement mortar, New Build Mater. (2004) 29–31.

[41] P.M. Wang, G.F. Zhang, Y.M. Zhang, Influence of polymer powders on mechanical properties of cement mortar, New Build Mater. 1 (2005) 32–36.

[42] M. Ramli, A.A. Tabassi, K.W. Hoe, Porosity, pore structure and water absorption of polymer-modified mortars: An experimental study under different curing conditions,

Compos. Part B Eng. 55 (2013) 221–233.

[43] M. Ramli, A.A. Tabassi, Mechanical behaviour of polymer-modified ferrocement under different exposure conditions: an experimental study, Compos. Part B Eng. 43 (2012) 447–456.

[44] N.B. Singh, S. Rai, Effect of polyvinyl alcohol on the hydration of cement with rice husk ash, Cem. Concr. Res. 31 (2001) 239–243.

[45] C.D. Anderson, E.S. Daniels, Emulsion polymerisation and latex applications, iSmithers Rapra Publishing, 2003.

[46] H. Althues, J. Henle, S. Kaskel, Functional inorganic nanofillers for transparent polymers, Chem. Soc. Rev. 36 (2007) 1454–1465.

[47] S. Zhong, Z. Chen, Properties of latex blends and its modified cement mortars, Cem. Concr. Res. 32 (2002) 1515–1524.

[48] S. Zhong, M. Shi, Z. Chen, The AC response of polymer-coated mortar specimens, Cem. Concr. Res. 32 (2002) 983–987.

[49] S. Ahmad, Reinforcement corrosion in concrete structures, its monitoring and service life prediction—a review, Cem. Concr. Compos. 25 (2003) 459–471.

[50] Y. Nakayama, Development of novel aqueous coatings which meet the requirements of ecology-conscious society: novel cross-linking system based on the carbonyl–hydrazide reaction and its applications, Prog. Org. Coatings. 51 (2004) 280–299.

[51] X. Zhang, Y. Liu, H. Huang, Y. Li, H. Chen, The diacetone acrylamide crosslinking reaction and its control of core-shell polyacrylate latices at ambient temperature, J. Appl. Polym. Sci. 123 (2012) 1822–1832.

[52] M.L. Picchio, M.C.G. Passeggi Jr, M.J. Barandiaran, L.M. Gugliotta, R.J. Minari, Waterborne acrylic–casein latexes as eco-friendly binders for coatings, Prog. Org. Coatings. 88 (2015) 8–16.

[53] Y. Ohama, Polymer-based admixtures, Cem. Concr. Compos. 20 (1998) 189–212.

[54] J. Machotová, E. Černošková, J. Honzíček, J. Šňupárek, Water sensitivity of fluorine-containing polyacrylate latex coatings: Effects of crosslinking and ambient drying conditions, Prog. Org. Coatings. 120 (2018). https://doi.org/10.1016/j.porgcoat.2018.03.016.

[55] N. Kessel, D.R. Illsley, J.L. Keddie, The diacetone acrylamide crosslinking reaction and its influence on the film formation of an acrylic latex, J. Coatings Technol. Res. 5 (2008) 285–297.

[56] ČSN EN 197-1 (722101), Cement - Část 1: Složení, specifikace a kritéria shody cementů pro obecné použití, 2013.

[57] T.S. EN, 196-1. Methods of testing cement–Part 1: Determination of strength, Eur. Comm. Stand. 26 (2005).

[58] M. Li, X.S. Lin, X.Y. Li, H.Q. Wang, Preparation and property study of core-shell ambient-temperature crosslinkable polyacrylate binder, in: Appl. Mech. Mater., Trans Tech Publ, 2014: pp. 3–6.

[59] J. Zhang, M. Yang, Y. Zhu, H. Yang, Synthesis and characterization of crosslinkable latex with interpenetrating network structure based on polystyrene and polyacrylate, Polym. Int. 55 (2006) 951–960.

[60] European Comitee for Standardization (CEN), EN 12390-1, Testing hardened concrete - Part 1: Shape, dimensions and other requirements for specimens and moulds., 2013.

[61] J. Machotová, A. Kalendová, D. Steinerová, P. Mácová, S. Šlang, J. Šňupárek, J. Vajdák, Water-Resistant Latex Coatings: Tuning of Properties by Polymerizable Surfactant, Covalent Crosslinking and Nanostructured ZnO Additive, Coatings. 11 (2021) 347.

[62] ČSN EN ISO 3251 (673031) Nátěrové hmoty - Stanovení netěkavých podílů

nátěrových hmotách a pojivech pro nátěrové hmoty, 2003.

[63] ISO 2115:1996 Plastics — Polymer dispersions — Determination of white point temperature and minimum film-forming temperature, 1996.

[64] ČSN EN ISO 2555 (640346) Plasty - Pryskyřice v kapalném, emulgovaném nebo dispergovaném stavu - Stanovení zdánlivé viskozity použitím rotačního viskozimetru s jednoduchým válcem, 2019.

[65] ČSN EN ISO 6427 Plasty - Stanovení látek extrahovatelných organickými rozpouštědly (konvenční metody), 2014.

[66] European Comitee for Standardization (CEN), EN 933-1, Test of geometrical properties of aggregate – Part 1: Determination of particle size distribution – Sieving method., 2012.

[67] ČSN EN 1015-3 (722400) Zkušební metody malt pro zdivo - Část 3: Stanovení konzistence čerstvé malty (s použitím střásacího stolku), 2000.

[68] ČSN EN 1015-10 (722400) Zkušební metody malt pro zdivo - Část 10: Stanovení objemové hmotnosti suché zatvrdlé malty, 2000.

[69] 2007, ČSN EN 1936 (721143) Zkušební metody přírodního kamene - Stanovení měrné a objemové hmotnosti a celkové a otevřené pórovitosti, n.d.

[70] J. Pokorný, R. Ševčík, J. Šál, L. Zárybnická, J. Žák, Lightweight Concretes with Improved Water and Water Vapor Transport for Remediation of Damp Induced Buildings, Materials (Basel). 14 (2021) 5902.

[71] ČSN EN 1015-18 (722400) Zkušební metody malt pro zdivo - Část 18: Stanovení koeficientu kapilární absorpce vody v zatvrdlé maltě, 2003.

[72] J. Lu, K. Wang, M.-L. Qu, Experimental determination on the capillary water absorption coefficient of porous building materials: A comparison between the intermittent and continuous absorption tests, J. Build. Eng. 28 (2020) 101091.

[73] M.K. Kumaran, Moisture diffusivity of building materials from water absorption measurements, J. Therm. Envel. Build. Sci. 22 (1999) 349–355.

[74] K. Scrivener, A. Ouzia, P. Juilland, A.K. Mohamed, Advances in understanding cement hydration mechanisms, Cem. Concr. Res. 124 (2019) 105823.

[75] L. Zárybnická, J. Machotová, P. Mácová, D. Machová, A. Viani, Design of polymeric binders to improve the properties of magnesium phosphate cement, Constr. Build. Mater. 290 (2021) 123202.

[76] H.B. Wagner, Polymer-modified hydraulic cements, Ind. Eng. Chem. Prod. Res. Dev. 4 (1965) 191–196.

[77] Y. Ohama, Principle of latex modification and some typical properties of latex-modified mortars and concretes adhesion; binders (materials); bond (paste to aggregate); carbonation; chlorides; curing; diffusion, Mater. J. 84 (1987) 511–518.

[78] P.W. Brown, E. Franz, G. Frohnsdorff, H.F.W. Taylor, Analyses of the aqueous phase during early C3S hydration, Cem. Concr. Res. 14 (1984) 257–262.

[79] S. Baueregger, M. Perello, J. Plank, Influence of carboxylated styrene–butadiene latex copolymer on Portland cement hydration, Cem. Concr. Compos. 63 (2015) 42–50.

[80] T.F. Sevelsted, J. Skibsted, Carbonation of C–S–H and C–A–S–H samples studied by 13C, 27Al and 29Si MAS NMR spectroscopy, Cem. Concr. Res. 71 (2015) 56–65.

[81] M. Auroy, S. Poyet, P. Le Bescop, J.-M. Torrenti, T. Charpentier, M. Moskura, X. Bourbon, Comparison between natural and accelerated carbonation (3% CO2): Impact on mineralogy, microstructure, water retention and cracking, Cem. Concr. Res. 109 (2018) 64–80.

[82] M.H.H. Mahmoud, M.M. Rashad, I.A. Ibrahim, E.A. Abdel-Aal, Crystal modification of calcium sulfate dihydrate in the presence of some surface-active agents, J. Colloid Interface Sci. 270 (2004) 99–105.

[83] S. Lv, J. Liu, T. Sun, Y. Ma, Q. Zhou, Effect of GO nanosheets on shapes of cement hydration crystals and their formation process, Constr. Build. Mater. 64 (2014) 231–239.

[84] H.A. Kharazian, M.R. Zare, M. Noktehdan, A. Sedaghatdoost, Effect of water-based acrylic copolymer on void systems of cementitious repair mortar, Case Stud. Constr. Mater. 11 (2019) e00261.

[85] Y.-Y. Kim, K.-M. Lee, J.-W. Bang, S.-J. Kwon, Effect of W/C ratio on durability and porosity in cement mortar with constant cement amount, Adv. Mater. Sci. Eng. 2014 (2014).

[86] B. Łaźniewska-Piekarczyk, Examining the possibility to estimate the influence of admixtures on pore structure of self-compacting concrete using the air void analyzer, Constr. Build. Mater. 41 (2013) 374–387.

[87] S.I. Karakashev, M. V Grozdanova, Foams and antifoams, Adv. Colloid Interface Sci. 176 (2012) 1–17.

[88] L.M. Saija, Waterproofing of portland cement mortars with a specially designed polyacrylic latex, Cem. Concr. Res. 25 (1995) 503–509.

[89] M. Wang, R. Wang, H. Yao, S. Farhan, S. Zheng, Z. Wang, C. Du, H. Jiang, Research on the mechanism of polymer latex modified cement, Constr. Build. Mater. 111 (2016) 710–718.

[90] J.A. Rossignolo, M.V.C. Agnesini, Mechanical properties of polymer-modified lightweight aggregate concrete, Cem. Concr. Res. 32 (2002) 329–334.

[91] H. Wu, B. Huang, X. Shu, Q. Dong, Laboratory evaluation of abrasion resistance of portland cement pervious concrete, J. Mater. Civ. Eng. 23 (2011) 697–702.

[92] N.N.A. Tukimat, N.N. Sarbini, I.S. Ibrahim, C.K. Ma, K. Mutusamy, Fresh and Hardened State of Polymer Modified Concrete and Mortars - A Review, MATEC Web

Conf. 103 (2017). https://doi.org/10.1051/matecconf/201710301025.

[93] M. Ismail, B. Muhammad, J.M. Yatim, A.H. Noruzman, Y.W.O.O. Soon, Behavior of concrete with polymer additive at fresh and hardened states, Procedia Eng. 14 (2011) 2230–2237.

[94] J. Machotova, S. Podzimek, P. Kvasnicka, H. Zgoni, J. Snuparek, M. Cerny, Effect of molar mass on film-forming properties of self-crosslinking latexes based on structured acrylic microgels, Prog. Org. Coatings. 92 (2016) 23–28.

[95] Y. Tian, X. Jin, N. Jin, R. Zhao, Z. Li, H. Ma, Research on the microstructure formation of polyacrylate latex modified mortars, Constr. Build. Mater. 47 (2013) 1381–1394. https://doi.org/10.1016/j.conbuildmat.2013.06.016.

[96] P.K. Mehta, Concrete. Structure, properties and materials, (1986).

[97] M. Jamshidi, H.R. Pakravan, K. Zojaji, Correlation between water permeability of latex-modified concrete (LMC) and water diffusion coefficient of latex film, Iran. Polym. J. 22 (2013) 799–809.

[98] E. Knapen, D. Van Gemert, Polymer film formation in cement mortars modified with water-soluble polymers, Cem. Concr. Compos. 58 (2015) 23–28. https://doi.org/10.1016/j.cemconcomp.2014.11.015.

[99] N.S. Martys, C.F. Ferraris, Capillary transport in mortars and concrete, Cem. Concr. Res. 27 (1997) 747–760.

[100] B. Liu, J. Shi, M. Sun, Z. He, H. Xu, J. Tan, Mechanical and permeability properties of polymer-modified concrete using hydrophobic agent, J. Build. Eng. 31 (2020) 101337.